Flexible and Printed Electronics



# Feasibility of conductive embroidered threads for $I^2C$ sensors in microcontroller-based wearable electronics



IOP Publishing Flex. Print. Electron. 8 (2023) 015016 https://doi.org/10.1088/2058-8585/acbbdc

Flexible and Printed Electronics



OPEN ACCESS

RECEIVED
18 November 2022

REVISED
20 January 2023

ACCEPTED FOR PUBLICATION
14 February 2023

PUBLISHED
27 February 2023



PAPER

# Feasibility of conductive embroidered threads for I$^2$C sensors in microcontroller-based wearable electronics

**Gabriele Volpes**[1,3], **Simone Valenti**[1,3], **Hima Zafar**[2,3], **Riccardo Pernice**[1] and **Goran M Stojanović**[2,*]

[1] Department of Engineering, University of Palermo, Viale delle Scienze, Building 9, Palermo 90128, Italy
[2] Department of Power, Electronics and Telecommunication Engineering, Faculty of Technical Sciences, University of Novi Sad, 21000 Novi Sad, Serbia
[3] These authors contributed equally to this work.
[*] Author to whom any correspondence should be addressed.

**E-mail:** sgoran@uns.ac.rs

**Keywords:** textile electronics, conductive threads, I$^2$C communication protocol, wearable health devices (WHDs), photoplethysmography (PPG)

Supplementary material for this article is available online

## Abstract

In recent years, the importance of flexible and textile electronics in the field of wearable devices has continuously increased, as they are expected to replace conventional wires that exhibit limited resistance to the mechanical stress occurring in on-body applications. Wearable health devices (WHDs) can provide physiological information about various body parts and employ distributed sensor networks. Among the sensors typically integrated within WHDs, those based on the I$^2$C communication protocol are very common and exploit signals transmitted at frequencies up to hundreds of kilohertz. Therefore, robust communication is required to guarantee a proper transmission of the signal at those frequencies. In this context, we have realized embroidered conductive threads exhibiting a lower resistance, appositely designed to replace conventional wires in a microcontroller-based wearable device employing I$^2$C sensors. A commercial conductive thread (silver coated polyamide) was used to embroider the conductive lines on to cotton fabric. Preliminary measurements were performed to characterize the response of these materials to signals typically operated within the I$^2$C communication protocol at different path lengths. Resistive measurements have also been performed to stimulate different environmental conditions, that is, temperature, the effect of sweating, and repeated washing cycles, also apply mechanical stress, i.e. twisting, with promising results that validate our conductive paths for digital signal communication.

## 1. Introduction

The technological advancements that have made possible the seamless integration, multifunctionality, customizability, and robustness of flexible electronics in wearable devices have attracted the interest of researchers in e-textiles, which integrate smart electronics with lightweight and breathable textiles [1, 2]. Indeed, the increasingly widespread use of wearable solutions, particularly in the biomedical field, necessitates the development of novel technologies for the fabrication of miniaturized and high-performance wearable devices in order to improve their dependability and comfort during daily use. Although huge strides have been taken towards the scalability of wearable sensors [3–5] most of these devices continue to employ common copper wires, whose characteristics in terms of mechanical strength (i.e. fracture and fatigue) limit their use in a wearable context [6, 7]. Therefore, it is necessary to investigate alternative communication technologies for replacing such wires with flexible solutions more suitable for wearable use.

In this context, conductive fibers are a significant component in e-textiles because they can provide electrical capabilities to electronic devices without

compromising the unique properties of textiles. The practicality of conductive fibers in commercial wearable health devices (WHDs) and broad consumer products has to be investigated, with the primary concerns being robustness and flawless integration.

To integrate conductive threads onto fabrics substrate 'embroidery techniques' have emerged as a promising method for fabricating textile-based circuits for smart wearables, due to the greater freedom in circuit design and relatively simple manufacturing that they provide over other processes like weaving, knitting, and printing [8]. By combining conductive threads and a computer numerically controlled embroidery machine, circuits may be quickly and simply designed. Once the textile conductive threads have been developed, it is quite intuitive to foresee their integration within WHDs. These electronic systems, indeed, can easily employ conductive paths as a data bus, being the latter used to enable communication with analog and digital integrated sensors implementing different digital communication protocols, also dedicating other conductive paths for power supply. As a matter of fact, incorporating electronic circuits into clothing through stitched connections would allow to increase their flexibility and personalization, thus making them even more comfortable, suitable to be worn and used in daily-life situations.

The motivation of this study is to develop a way for integrating sensors and fabrics. One straight forward approach is wireless communication. Each sensor operates with a tiny battery and sends data over the cloud network. However, frequent data transmission by densely distributed sensors will involve significant difficulties including interference, latency, and battery life [9]. Another approach is based on the wired communication, in which inter-integrated circuit ($I^2C$) serial communication protocol is used to power and transmit data on a conductive fabric material.

$I^2C$, indeed, is one of the most commonly employed protocols in WHDs thanks to the fact that it exploits just two different lines to synchronously transmit data between slaves and masters, thus allowing for the integration of a large number of sensors and devices. These two lines, called serial data (SDA) and serial clock (SCL), are respectively used to transmit data in both directions and to share a clock generated by the master [10, 11]. Among all the integrated sensors used in wearable context, photoplethysmographic (PPG) ones represent the most widely employed sensors integrated within WHDs and exploiting the $I^2C$ communication protocol, given the high level of contribution they can provide. These sensors, in fact, are usually exploited to extract, through optical signals, useful information on the health status of the cardiovascular system of an individual. Specifically, the optical beam emitted by the light source penetrates through the body part (e.g. the fingertip) before being acquired by the photodetector. The change in absorbance is used to calculate not only parameters such as oxygen saturation, heart rate, respiratory rate, hypo- and hypervolemia, but also to estimate blood pressure and stress level [12–17].

In this paper, we investigate the feasibility study focused on the use of conductive textile threads in place of conventional copper wires for replacing $I^2C$ lines (i.e. SDA and SCL) for the future wearable application of hand glove. To avoid conductive path malfunctioning, we investigated possible environmental conditions and analyzed the effect on e-textile performances in terms of change in electrical resistance as well as digital signals. The innovative aspects of this work can be summarized as follows: (a) analyzing different lengths of the conductive textile paths in order to confirm the functionality of the electrical circuit and bio-signal transmission, (b) the performances of the embroidered textile lines have been characterized as a function of temperature changes, applying artificial sweat to it, during washing test and applying mechanical stress (i.e. twisting) in order to assess the robustness of signal transmission, (c) these measurements have been carried out using an $I^2C$ PPG sensor in reflection mode, where the PPG signal measurement has been performed during the execution of the experimental protocols to validate the proper data transmission.

## 2. Materials and methods

### 2.1. Design and realization of embroidered sample

For this experiment, a commercial conductive thread, Silver-tech 100, supplied by AMANN Group, Germany [18], was used to embroider the conductive lines on to the cotton fabric (thickness = 0.14 mm). Silver-tech 100 is a silver-coated polyamide continuous filament with a linear mass density of 110 × 3 dtex, an optical diameter of 0.2 mm, $<200\ \Omega\ m^{-1}$ according to the datasheet provided by the company.

According to the literature [19] conductive yarns can be obtained by melt-spinning or wet-spinning technologies, where it is possible to mix different polymers and fillers, extruding them together into a composite yarn. These silver conductive threads can get oxidized over time, but oxidization is a very mild and slow process which also depends on the thickness of silver coating, as evidenced in [20]. For this reason, freshly ordered spool of conductive yarn was used in this experiment, and we did not noticed any silver oxidation during our study.

For embroidery an industrial technical embroidery machine was used (Model-JCZA 0109-550, ZSK, Germany). Firstly, interconnecting lines were drawn

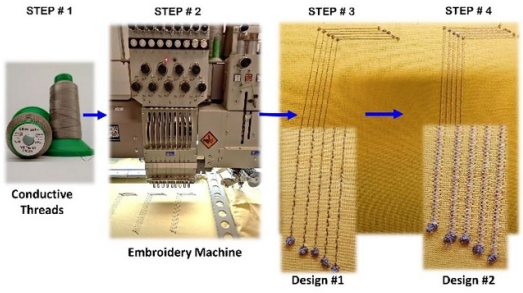


**Figure 1.** Schematic representation of step-by-step process of embedding conductive yarns into textile through embroidering technique.

**Table 1.** Specification of material used for making embroidered conductive path.

| Material | Yarn count | Composition | Resistance |
|---|---|---|---|
| Silver-coated conductive yarn (Silver Tech 100) | 110 × 3 dtex, 91/3 Nm | 100% polyamide/silver coated | $<200\ \Omega\ m^{-1}$ |
| White Burmilon No.120/2 | 98 × 2 dtex, 102/2 Nm | 100% polyester thread | — |
| Bobby Maxi-100 | 80 × 2 dtex | 100%polyester thread | — |

with accurate measurements of hand with a total length of 17 cm and a stitch length of 0.5 mm, in stitch digitizing program (Gis BasePac 10, ZSK, Germany), referred as 'Design #1' in figure 1.

In the last step, non-conductive thread (White Burmilon No.120/2, 100% polyester thread by Madeira, UK) was used to cover/coat the embroidered Design#1, in order to protect it from short circuiting or environmental effects (e.g. temperature, humidity, etc) or giving it extra mechanical strength, referred as 'Design #2' in figure 1. The particular parameters used in GIS Base Pac software were 'swing & shift running line', with zig-zag stich length of 2 mm crossing over/above the interconnecting line.

Cotton fabric was used as base material for embroidered connection lines due to its high absorption of both water and moisture. It exhibits a high degree of air permeability and very effective heat transference.

The bottom bobbin thread used throughout the design was bobby Maxi-100, 100% polyester thread, by Gunold Company, Portugal. The reason for using nonconductive thread in the bottom/backside/other side of the fabric is to actually avoid skin interference with the embroidered design. Soak test was also conducted to confirm the statement made previously. Preliminary results are included in supplementary material, figure S4.

Table 1 summarizes the specifications of the material throughout the experiment.

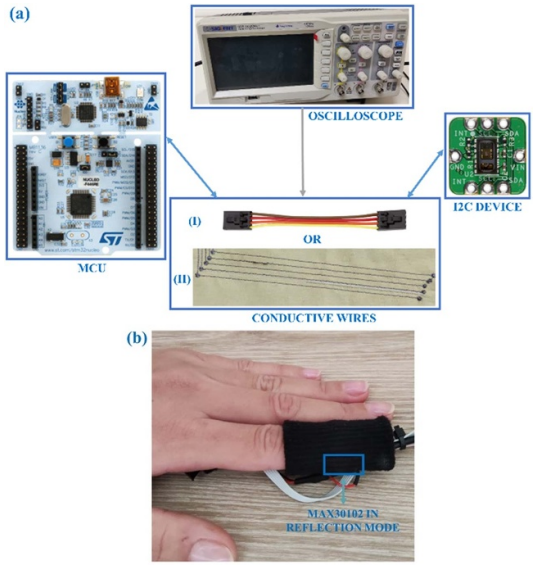


**Figure 2.** (a) An illustration of the experimental set up: the microcontroller shares SDA and SCL signals to $I^2C$ device by two separate $I^2C$ ports using commercial copper (I) and embroidered (II) wires, acquiring signals present in both lines with oscilloscope; (b) A detail of the PPG signal acquisition.

### 2.2. Experimental protocol

Figure 2 depicts the experimental set-up used in this work to evaluate digital transmission employing embroidered threads. For this experiment, the microcontroller used was STM32F446RE implemented on a Nucleo-64 development board; it was connected via $I^2C$ communication protocol, with $I^2C$ speed set to 100 kHz, to MAX30102, manufactured by Maxim Integrated. This sensor allows to acquire PPG waveforms in reflection mode (i.e. configuration with the light source and the photodetector placed on the same side of the measured human tissue) using two LEDs that emit light at two different wavelengths, i.e. 660 nm (red) and 880 nm (infrared), with an ambient light cancellation front-end and an up to 18-bit ultra-low noise analog-to-digital converter.

Signals acquired from SCL, and SDA lines were displayed in real-time on a digital oscilloscope (Siglent SDS 1102 CML+) with 8-bit vertical resolution [21]. Measurements were carried out on the left forefinger of a 28 year-old healthy female volunteer for about 30 s during a rest condition where the subject, in a sitting position, was asked to breathe normally and stay relaxed. The signal received from a PPG sensor was acquired through the $I^2C$ communication protocol interconnected to a microcontroller, with common copper cables (flat cables), and flexible embroidered threads realized for this purpose. The measurements were then repeated on double and triple-length embroidered paths in order to evaluate the quality of the digital transmission as the length of the conductive thread increases. Signals were recorded at a sampling rate of 1 MHz and stored on a

USB flash drive in order to visualize and post-process them using MATLAB R2022a (The MathWorks, Inc., Natick, MA, USA) software [22].

### 2.3. Measurements and evaluation methodology

To evaluate the influence of environmental conditions on digital signals, an electrical impedance spectroscopy (EIS) method was implemented using the PalmSens4 device used to measure resistance, which was extracted from impedance values obtained from the device. The potential was set at 0.01 V, the frequency range was 1 Hz–100 kHz, and 51 logarithmically spaced samples were taken. In this study, we specifically focused on four significant environmental factors that can seriously damage the conductive embroidered path, i.e. (a) temperature, (b) sweat, (c) washing and (d) twisting.

To evaluate the influence of temperature on digital signals, a bench top heater was used to increase the temperature of the embroidered path. To monitor and control the temperature, a thermal camera was used to focus on the threads. The starting temperature was 20 °C (room temperature), which was then increased at steps of 10 °C up to 60 °C. Every 10 min, the resistance was checked.

The artificial sweat solution used was prepared according to the method reported in [23], with a pH of 6.5 to emulate the behavior of sweat during daily-use of the device. Resistance measurements were carried out by gradually applying a solution with increasing amounts of artificial sweat (100–400 $\mu$l) through a pipette to a specific small portion of the embroidered path, waiting for five minutes until the solution was totally absorbed by the fabric. The time duration was set in accordance with the standard BS 4554:1970, which represents the method of testing for the wettability of textile fabrics.

For a better understanding of research methodology, the experimental setup used in this study for simulating sweating conditions was shown in figure 3.

In the third round of the experiment, the washing test was carried out five times, in order to replicate a real-life application scenario. In accordance with ISO 6330:2012, fabric domestic washing and drying procedures were applied for this test. Following the methodology described in [24], we did not use any detergent, as we just wanted to test 'water stress', since the conductive threads may react differently when use detergent or bleaching agent as mentioned by the manufacturer [18]. The fabric was simply washed with tap water and left to dry at room temperature (25 °C). A fully dry condition was recorded using a digital multi-meter and thermal camera until the next measurement was taken.

Mechanical stress is one of the most detrimental aspects of smart textile constructions. This is especially true for conductive yarns which are used for the connection between the conductive yarn and the electronic component in e-textile [25]. To validate that, in the fourth round of experiment, only twisting was done, given that stretching and friction test are not needed in our application of hand glove. The twisting was performed five times (where one twist equals to 180°), until material could not twist anymore.

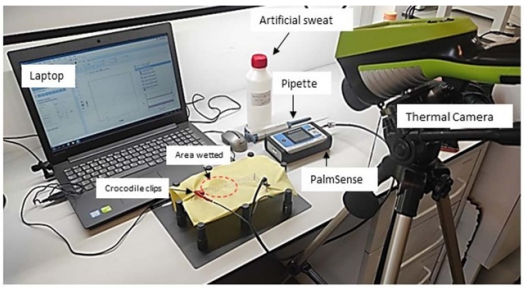


**Figure 3.** Experimental setup for artificial sweat application on the fabric, including impedance analyzer, thermal camera, computer, pipette, artificial sweat, and fabric.

### 2.4. Sample preparation of artificial sweat

The artificial sweat solution was prepared according to the method reported in [26], with a pH of 6.5 and with following [27] concentration of: lactic acid $1.4 \times 10^{-2}$, glucose $1.7 \times 10^{-4}$, urea $1.0 \times 10^{-2}$, ascorbic acid $1.0 \times 10^{-5}$ mixed in deionized water according to the analyte content of human sweat.

## 3. Results and discussion

In order to validate the use of our embroidered threads for $I^2C$ communication, SCL and SDA signals were acquired via digital communication between two separate $I^2C$ microcontroller ports and the $I^2C$ sensor, simultaneously using commercial copper wires in the first $I^2C$ port and our embroidered paths in the second one. In this section, we describe the results of the measurements of SCL and SDA signals acquired using both commercial copper wires and embroidered paths at different lengths in order to visually assess the quality of digital signals obtained with both conductive technologies.

Figure 4 shows a 200 $\mu$s excerpt window of the SCL signal acquired from the oscilloscope using copper wire (blue) and embroidered thread (orange) on the SCL line shared by the microcontroller and $I^2C$ device during data exchange. Results evidence that SCL waveforms are perfectly overlapping in time, both showing a very stable clock signal of 100 kHz. Different results are observed with regard to the amplitudes of the two signals. Indeed, although both signals reach the high logical level of 3.3 V, the low logical level reached by the SCL signal evaluated on the embroidered path is approximately 0.5 V, higher

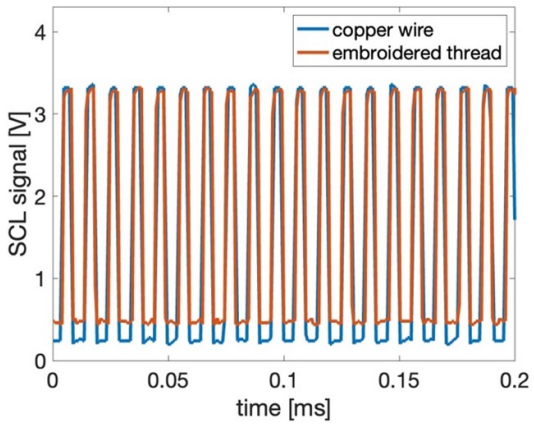


**Figure 4.** A 200 $\mu$s SCL signal acquisition window using copper wire (blue) and embroidered conductive silver thread (orange).

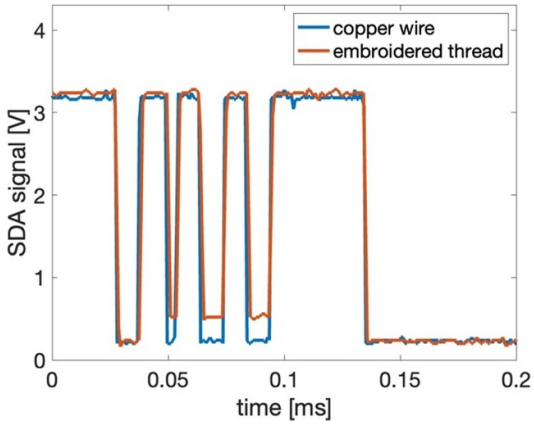


**Figure 5.** A 200 $\mu$s SDA signal acquisition window using copper wire (blue) and embroidered thread (orange).

than the 0.25 V measured on the copper wire. Nevertheless, both SCL waveforms are stable and free of significant noise, showing characteristics in line with those required by the clock signal used in $I^2C$ communication.

Figure 5 depicts the results of the measurements of two SDA signals during the communication between the microcontroller and $I^2C$ device of a present data package consisting of a message sent by the microcontroller to announce the start of the data exchange. Even in this case it is possible to notice a very strong agreement between the two waveforms, whose data sending is performed synchronously according to the clock signal present on the SCL line previously discussed in figure 4.

The comparison between the two SDA waveforms highlights, also in this case, that the low logical level of the signal present on the embroidered thread is higher than that measured on the copper wire, standing again at about 0.5 V. Moreover, figure 5 shows that the low logical level of the SDA signal on the embroidered thread is not well defined and sometimes reaches the same value achieved on the copper wire. This can be attributed to the speed at which both signals switch from the high logical level to the low one, which are due respectively to the bit rate in the case of the SDA signal and to the clock frequency in the case of the SCL signal. In fact, this behavior is observed only when the changes of the logical value occur after a short time amount, e.g. during the transmission of the SDA data packet (figure 5) or during the clock signal sharing (figure 4). On the other hand, the optimal low logical level (0.25 V) is reached whenever the signal remains at the high logical level for a longer period (i.e. respectively after the first and last high logical level reached by the SDA signal on figure 5). Besides, there are no differences in the high logical level, which maintains the same value of 3.3 V for both signals. Indeed, the fact that the high logical level always reaches the maximum voltage level is an expected behavior of the $I^2C$ protocol. In fact, when transmitting a 'logical 1', the SDA line is brought to the same level as the power supply voltage without current flowing on the line and, therefore, without any generation of voltage drop on the embroidered path.

The voltage drop detected in the embroidered path during every low logical level communication event, shown for both SCL and SDA signals (figures 4 and 5), is the only characteristic that distinguishes the waveforms present on the two lines, highlighting the only limit of our technology if compared to standard copper wires. This may be ascribed to the presence of residual potentials leading to a consequent decrease in thresholds for high/low logical levels distinction, thus resulting in a worsening of communication in terms of noise immunity that under certain noisy conditions could compromise the correct bitstream communication.

Nonetheless, the presence of residual potential is a phenomenon that we expect, since the embroidered path, although it may be composed of conductive material, has a resistance that is far from negligible, as discussed in the section 2. Despite this, a voltage drop of 0.5 V falls largely within the present low voltage threshold of the $I^2C$ protocol, which stands at a limit value of 1 V [28], making the resistive nature of our conductive path negligible for this application.

### 3.1. Impact on signal with increasing length of conductive paths

Figure 6 depicts the results of the measurements of SDA and SCL signal at different lengths of the embroidered path Specifically, being '*L*' the length of the original embroidered path used for the experiment (whose length, as specified in section 2.2, is 17 cm), we have carried out measurements of both signals at *L, 2 l* (i.e. 34 cm) and *3 l* (i.e. 51 cm)

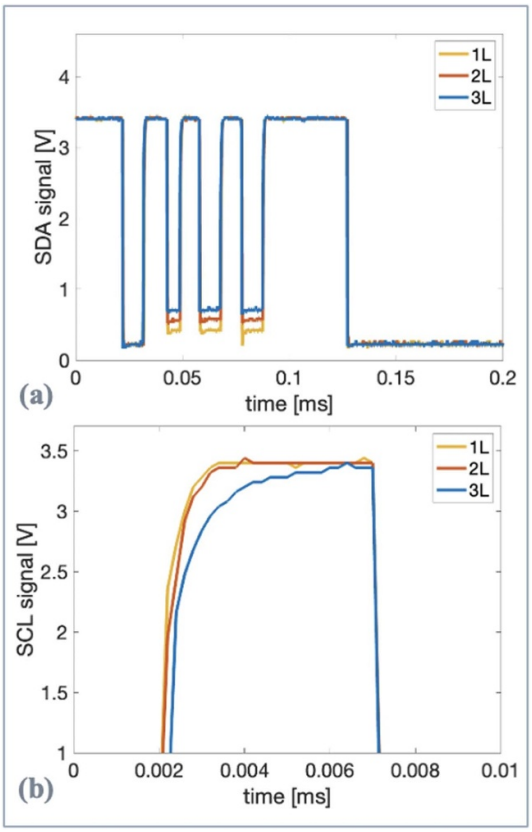


**Figure 6.** (a) A 200 $\mu$s SDA signal acquisition window (a) and a detail of the SCL waveform (b) obtained both using embroidered thread (yellow line), then repeating the measurements on double (orange line) and triple (blue line)-length embroidered threads.

embroidered threads in order to visually evaluate at what extent the length of the conductive threads affects the overall quality of the communication. As shown in figure 6(a), the SDA signal continues to exhibit the same behavior as discussed with regard to figure 5. In detail, the high logical level of the SDA signal remains unchanged regardless of the length of the conductive path, while the low logical level reached is different, increasing with the length of the conductive path. This behavior is expected and can be easily explained by considering the resistance of the conductive path as a function of length. In fact, as the latter increases, the resistance also rises, resulting in a voltage drop on the conductive thread proportional to its resistance value. This potential drop will be subtracted from the voltage value for the low logical level, explaining different trends observed in figure 6(a) at varying conductive path lengths.

Figure 6(b) shows a detail of the rising front of the clock signal shared on the SCL pin, also at varying embroidered path lengths (*L, 2 l* and *3 l*). The length of the conductive thread also affects the clock of the $I^2C$ protocol. In fact, the shape of the SCL signal changes for the three different embroidered paths length. In particular, as the length increases, the SDA waveform becomes increasingly smoothed, resulting in a general deterioration of the signal, moving away from the typical square wave-shape that a clock signal should exhibit in order to be correctly interpreted by all the devices involved in data communication.

Although similar, this behavior can be explained by considering the impedance (and not only resistance, as in the afore-mentioned case) of the conductive threads as a function of length. In fact, it is possible to observe two distinct behaviors caused both by the increase in length: the first is always due to the increase in resistance with the path length, which causes a voltage drop that limits the high logical level to a gradually lower voltage value, which is more evident in the SCL signal measured on the longest path (figure 6, blue line); the second is due to the occurrence of parasitic capacitive components of the material constituting the embroidered path that cannot longer be neglected, considering the typical hundreds kHz frequencies of $I^2C$ protocol together with the increasing path length. This produces the smoothed shape of the SCL signal which is an index of capacitive charging processes occurring in the conductive path under consideration.

Nevertheless, both SDA and SCL signals continue to show suitable characteristics for digital communication, since $I^2C$ data transmission between microcontroller and $I^2C$ device has been successful for all the lengths of the considered conductive threads.

Finally, figure 7 displays a 10 s PPG excerpt acquired through the $I^2C$ device, whose values were first numerically converted and then sent to the microcontroller via $I^2C$ communication protocol using, once again, both copper wires (dotted blue) and embroidered threads (orange) for SCL and SDA lines. The perfect overlap of the two waveforms indicates that the same data packets were exchanged on both communication channels during the whole PPG measurement.

Besides, the correct data exchange is also suggested by observing the high quality of the physiological signal, since the main morphological features of the PPG signal waveform are clearly visible [12].

The SDA signal from $I^2C$ device and shared via the embroidered path has been correctly decoded by the microcontroller, as shown in figure 7 (i.e. the PPG signal), for the whole measurement duration, thus validating the use of embroidered threads for $I^2C$ communication. Such results highlight that embroidered threads can represent a suitable solution for wearable applications thanks to their flexible structures.

### 3.2. Impact of the environmental conditions on the performance of conductive path

Since our conductive path is purely resistive, as also observed from the device data, it exhibits no phase shift between voltage and current. Therefore, using

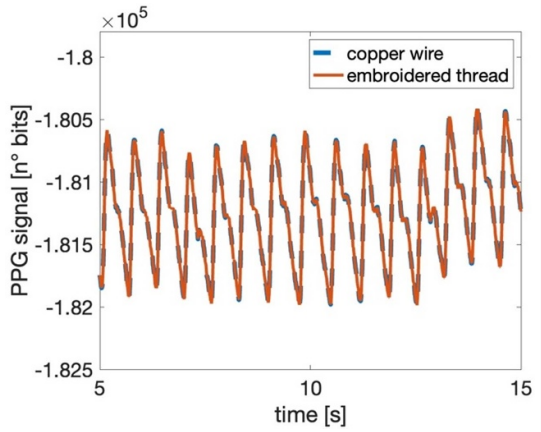


**Figure 7.** 10 s window of PPG signals acquired from I²C sensor in the same conditions using both copper wire (dotted blue) and embroidered thread (orange).

EIS method, we have plotted the graphs shown in this Subsection according to the following equation,

$$R = |Z| \cos \theta . \quad (1)$$

Figure 8(a) reports the trends of the resistance (Ω) as a function of temperature. The obtained results clearly demonstrate that temperature and resistance are inversely related: as the temperature goes up, the resistance of the conductive path linearly decreases [29]. A temperature increase, in theory, could melt the polyamide/polyamide-polyester core of the thread fibers and damage them, as reported in [30]. Interestingly, while continuously obtaining digital signals from operational sensors such as the PPG sensor through conductive paths channels, no heat generation is seen. The results can be found in supplementary document figure S5.

Figure 8(b) depicts the results in terms of variation of the resistance as a function of the amount of artificial sweat solution dropped onto the interconnecting line, since silver-coated yarn is affected by sweat. Despite the uniformity of the silver coating, which according to the threads datasheet is unaffected by water, the breaking of the silver coating on the surface of these threads allows the amide group to readily attach to water molecules, causing absorption and thus altering the internal resistance.

Figure 8(c) instead illustrates the variation of the resistance after up to five washing cycles. The characterization has been carried according to the reported works [31, 32] which also suggest that after the washing test some effects are observed on the conductive path due to sinners factors [33]. In our case (for further details see supplementary material, figure S1(C)) there is a combination of two parallels effects: the first one is due to shrinking of the conductive fiber, while the second one is due to silver coating removal. Due to repeated washing cycles, the coating

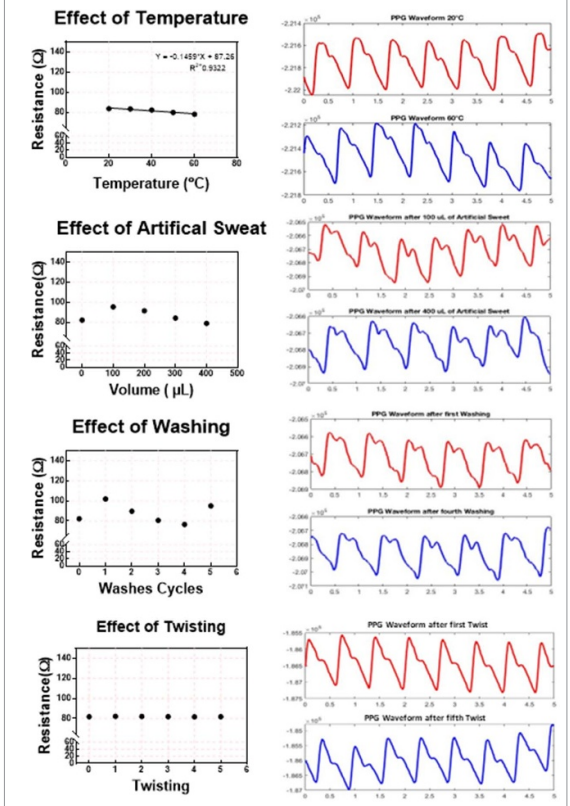


**Figure 8.** Variation of the resistance (a) at varying temperature, (b) by applying sweat solution, (c) after up to five washing cycles and (d) considering the effect of twisting. The left subplots show the resistance according to EIS method, while right subplots show the acquired PPG signal at two different conditions for each measurement type.

on the conductive path is removed, letting more water molecules to attach, which clearly shows after fourth washing increasing the resistance and decreasing the conductivity.

Finally, figure 8(d) show the result of twisting test which has been carried out as a part of mechanical stress to validate conductive path strength [34]. In particular, the twisting test did not produce any significant change in the resistance of the embroidered thread. Additionally, PPG acquisitions performed during the test did not show any signal corruption, as well-defined waveforms can be observed both under normal conditions and during the test. For each of these studies, surface analysis of conductive paths is shown in supplemental document figure S3, indicating that resistance increases are not caused by thread swelling. However, it is mostly affected by the silver plating peeling off.

The same behavior shown by the resistive impedance trend as a function of temperature is also found when applying artificial sweat. Instead, the trend after the washing test is more irregular, with a resistance decrease when undergoing first to fourth washing procedures, and then increasing again after the fifth

washing. Nonetheless, after each procedure (temperature, washing, and application of sweat solution), the correct signal transfer has been checked, suggesting that the device equipped with embroidered threads can operate well, even if it is washed five times, in temperature conditions ranging from 20 °C to 60 °C and sweat values produced by the surface in contact with the embroidered threads between 100 and 400 $\mu$l. Overall, our results highlight that resistance values (figure 8) range from 84 Ω to 78 Ω (with a variation of 7.1%) at varying temperatures, from 97 Ω to 79 Ω (with a decrease of 18.6%) when adding artificial sweat solution, and from 102 Ω to 78 Ω (with a variation of 23.5%) when undergoing the washing protocol.

Finally, no significant changes in resistance have been detected during the twisting test, highlighting the immunity of the material in response to mechanical stresses of this type. We additionally performed EIS spectrum analysis and results can be seen in figure S2 of the supplementary material. From graphs presented in figure S2, it can be concluded that the resistance of the silver threads is almost constant in a frequency range between 1 Hz and 100 kHz.

## 4. Conclusion

In this work, a feasibility study of replacing the common copper wires (flat cable) with embroidered conductive threads has been carried out. The acquisition protocol, which involves a comparison of the acquired signals, by interconnecting the sensors to the two separate $I^2C$ microcontroller ports using both common flat copper wires and embroidered conductive threads has been performed but did not show any differences in the PPG signals acquired. Nonetheless, when signals are acquired through tissue interconnections, an evident voltage drop is reported during zero logical level bit transmission in both SDA and SCL waveforms, caused by the non-negligible resistance of the embroidered path. This phenomenon, however, under our measurement conditions, does not compromise the proper signal transmission.

Preliminary results depict that it is possible to obtain, with the conductive thread solution, the same waveform as the one acquired with copper wires, with the strong advantage of using flexible threads that, thanks to their textile nature, are more suitable for use in wearable applications. Moreover, during temperature, sweating, and washing simulation protocols, a progressive decrease in resistance of conductive thread was observed, highlighting a good behavior to wear conditions that typically affect wearable devices. Future works may focus on the investigation of voltage drops in the low logical level of the signal and the conditions under which these could represent a limitation to the correct signal transmission. A future investigation could also foresee the replacement of the entire package of interconnections between microcontrollers and sensors, thus exploiting different communication protocols in order to investigate the robustness of these connections (i.e. CAN, UART and SPI) [35, 36].

## Data availability statement

The data that support the findings of this study are available upon reasonable request from the authors.

## Acknowledgments

The authors gratefully acknowledge funding from the European Union's Horizon 2020, WIDESPREAD-04-2019: ERA Chairs under Grant Agreement No. 854194 (STRENTEX: ERA Chair for emerging technologies and innovative research in Stretchable and Textile Electronic) http://strentexproject.com/, (accessed on 9 October 2022). GV PhD grant was supported by Istituto Nazionale Previdenza Sociale (INPS) PhD fellowship, project title 'Sviluppo di protocolli sperimentali e impiego di soluzioni tecnologiche finalizzate alla valutazione oggettiva e quantitativa dello stress lavoro-correlato'. SV PhD grant was supported by the Italian MIUR PON R&I 2014-2020 'Dottorati innovativi con caratterizzazione industriale' funding programme. R P was partially supported by European Social Fund (ESF)—Complementary Operational Programme (POC) 2014/2020 of the Sicily Region.

## Conflict of interest

The authors declare no conflict of interest.

## ORCID iDs

Gabriele Volpes https://orcid.org/0000-0003-1383-2896
Simone Valenti https://orcid.org/0000-0001-5259-8030
Riccardo Pernice https://orcid.org/0000-0002-9992-3221
Goran M Stojanović https://orcid.org/0000-0003-2098-189X

## References

[1] Iyer S V, George J, Sathiyamoorthy S, Palanisamy R, Majumdar A and Veluswamy P 2022 Pertinence of textile-based energy harvesting system for biomedical applications *J. Nanomater.* **2022** e7921479
[2] Radouchova M, Suchy S and Blecha T 2022 Embroidered flexible elastic textile antenna as strain sensor *2022 45th Int. Spring Seminar on Electronics Technology (ISSE)* pp 1–6
[3] Heikenfeld J *et al* 2018 Wearable sensors: modalities, challenges, and prospects *Lab Chip* **18** 217–48
[4] Patel S, Park H, Bonato P, Chan L and Rodgers M 2012 A review of wearable sensors and systems with application in rehabilitation *J. Neuroeng. Rehabil.* **9** 21
[5] Ates H C, Nguyen P Q, Gonzalez-Macia L, Morales-Narváez E, Güder F, Collins J J and Dincer C 2022

End-to-end design of wearable sensors *Nat. Rev. Mater.* **7** 887–907
[6] Gbur J L and Lewandowski J J 2016 Fatigue and fracture of wires and cables for biomedical applications *Int. Mater. Rev.* **61** 231–314
[7] Benini B J 2010 Tension and flex fatigue behavior of small diameter wires for biomedical applications *Case Western Reserve University* (available at: https://etd.ohiolink.edu/apexprod/rws_olink/r/1501/10?clear=10&p10_accession_num=case1269970809) (Accessed 27 October 2022)
[8] Ruckdashel R R, Khadse N and Park J H 2022 Smart E-textiles: overview of components and outlook *Sensors* **22** 16
[9] Ko J Wireless sensor networks for healthcare *IEEE Journals & Magazine IEEE Xplore* (available at: https://ieeexplore.ieee.org/abstract/document/5570866) (Accessed 19 January 2023)
[10] Chen Y, Xiao F, Yu L and Cui P 2020 Design of multi-line elastic belt conveying control system for knitting machine based on $I^2C$ protocol *IEEE Access* **8** 51803–9
[11] Righetti X and Thalmann D 2010 Proposition of a modular $I^2C$-based wearable architecture *undefined* (available at: www.semanticscholar.org/paper/Proposition-of-a-modular-I2C-based-wearable-Righetti-Thalmann/06588df5f1d9e24337709f00fddd47afaaa36cca) (Accessed 14 November 2022)
[12] Allen J 2007 Photoplethysmography and its application in clinical physiological measurement *Physiol. Meas.* **28** R1
[13] Lee H, Chung H, Ko H, Parisi A, Busacca A, Faes L, Pernice R and Lee J 2022 Adaptive scheduling of acceleration and gyroscope for motion artifact cancelation in photoplethysmography *Comput. Methods Programs Biomed.* **226** 107126
[14] Tusman G, Acosta C M, Pulletz S, Böhm S H, Scandurra A, Arca J M, Madorno M and Sipmann F S 2019 Photoplethysmographic characterization of vascular tone mediated changes in arterial pressure: an observational study *J. Clin. Monit. Comput.* **33** 815–24
[15] Loh H W, Xu S, Faust O, Ooi C P, Barua P D, Chakraborty S, Tan R-S, Molinari F and Acharya U R 2022 Application of photoplethysmography signals for healthcare systems: an in-depth review *Comput. Methods Programs Biomed.* **216** 106677
[16] Pernice R, Parisi A, Faes L, Busacca A, Adamo G and Guarino S 2019 A portable system for multiple parameters monitoring: towards assessment of health conditions and stress level in the automotive field *2019 AEIT Int. Conf. of Electrical and Electronic Technologies for Automotive (AEIT AUTOMOTIVE)* (available at: https://pure.unipa.it/en/publications/a-portable-system-for-multiple-parameters-monitoring-towards-asse) (Accessed 14 November 2022)
[17] Han H J, Labbaf S, Borelli J L, Dutt N and Rahmani A M 2020 Objective stress monitoring based on wearable sensors in everyday settings *J. Med. Eng. Technol.* **44** 177–89
[18] Special conductive thread by AMANN: silver-tech+ (available at: www.amann.com/products/product/silver-tech-plus/) (Accessed 10 October 2022)
[19] Bonaldi R R 2018 Electronics used in high-performance apparel—Part 1/2 *High-Performance Apparel* (Amsterdam: Elsevier) pp 245–84
[20] Kramar A 2013 Influence of structural changes induced by oxidation and addition of silver ions on electrical properties of cottonyarn *Cellul. Chem. Technol.* **48** 189–97
[21] Siglent SDS1102CML+100MHz Dual channel oscilloscope *siglent.eu.* (available at: www.siglent.eu/product/1139189/siglent-sds1102cml-100mhz-dual-channel-oscilloscope) (Accessed 16 November 2022)
[22] Blinowska K J and Żygierewicz J 2021 *Practical Biomedical Signal Analysis Using MATLAB®* 2nd edn (Boca Raton,FL: CRC Press) (https://doi.org/10.1201/9780429431357)
[23] Midander K, Julander A, Kettelarij J and Lidén C 2016 Testing in artificial sweat—is less more? Comparison of metal release in two different artificial sweat solutions *Regul. Toxicol. Pharmacol.* **81** 381–6
[24] Feng P-Y, Xia Z, Sun B, Jing X, Li H, Tao X, Mi H-Y and Liu Y 2021 Enhancing the performance of fabric-based triboelectric nanogenerators by structural and chemical modification *ACS Appl. Mater. Interfaces* **13** 16916–27
[25] Zaman S U Market readiness of smart textile structures—reliability and washability *IOPscience* (available at: https://iopscience.iop.org/article/10.1088/1757-899X/459/1/012071/meta) (Accessed 15 January 2023)
[26] We X Wearable biosensor for sensitive detection of uric acid in artificial sweat enabled by a fiber structured sensing interface *ScienceDirect* (available at: www.sciencedirect.com/science/article/pii/S2211285521002895?casa_token=stkvvhsfrWUAAAAA:jCRdBgj7UeObvR33GDnANMLl8uSnoSGjVwrAolokwO-TtuUgV4sGIahr7uukEpOoS5poRPIQPJ8) (Accessed 19 Janury 2023)
[27] Harvey C J, LeBouf R F and Stefaniak A B 2010 Formulation and stability of a novel artificial human sweat under conditions of storage and use *Toxicol. Vitro* **24** 1790–6
[28] Xyz A The 2 C-bus specification (available at: www.academia.edu/31040217/THE_I_2_C_BUS_SPECIFICATION_VERSION_2_1_JANUARY_2000_The_I_2_C_bus_specification) (Accessed 27 October 2022)
[29] Ding J T F, Tao X, Au W M and Li L 2014 Temperature effect on the conductivity of knitted fabrics embedded with conducting yarns *Text. Res. J.* **84** 1849–57
[30] Stavrakis A K, Simić M and Stojanović G M 2021 Electrical characterization of conductive threads for textile electronics *Electronics* **10** 8
[31] Rotzler S, Kallmayer C, Dils C, von Krshiwoblozki M, Bauer U and Schneider-Ramelow M 2020 Improving the washability of smart textiles: influence of different washing conditions on textile integrated conductor tracks *J. Text. Inst.* **111** 1766–77
[32] Afroj S, Tan S, Abdelkader A M, Novoselov K S and Karim N 2020 Highly conductive, scalable, and machine washable graphene-based E-textiles for multifunctional wearable electronic applications *Adv. Funct. Mater.* **30** 2000293
[33] Rotzler S and Schneider-Ramelow M 2021 Washability of E-textiles: failure modes and influences on washing reliability *Textiles* **1** 1
[34] Huang F Textiles free full-text review of fiber- or yarn-based wearable resistive strain sensors: structural design, fabrication technologies and applications (available at: www.mdpi.com/2673-7248/2/1/5) (Accessed 15 Janury 2023)
[35] Visconti P Features, operation principle and limits of spi and i2c communication protocols for smart objects: a novel spi-based hybrid protocol especially suitable for iot applications 2017 *Int. J. Smart Sens. Intell. Syst.* **10** 1–34
[36] Sharma S *et al* 2015 Review on CAN based Intercommunication between microcontrollers *J. emerg. technol. innov. res.* **2** 4